

## Supplementary Information

### High-pressure phase diagrams of $\text{FeSe}_{1-x}\text{Te}_x$ : Correlation between suppressed nematicity and enhanced superconductivity

K. Mukasa,<sup>1</sup> K. Matsuura,<sup>1</sup> M. Qiu,<sup>1</sup> M. Saito,<sup>1</sup> Y. Sugimura,<sup>1</sup>  
K. Ishida,<sup>1</sup> M. Otani,<sup>2</sup> Y. Onishi,<sup>2</sup> Y. Mizukami,<sup>1,2</sup> K. Hashimoto,<sup>1,2</sup>  
J. Gouchi,<sup>3</sup> R. Kumai,<sup>4</sup> Y. Uwatoko,<sup>3</sup> and T. Shibauchi<sup>1,2</sup>

<sup>1</sup>*Department of Advanced Materials Science,  
University of Tokyo, Kashiwa, Chiba 277-8561, Japan*

<sup>2</sup>*Department of Applied Physics, University of Tokyo, Hongo, Tokyo 113-8656, Japan*

<sup>3</sup>*Institute for Solid State Physics, University of Tokyo, Kashiwa, Chiba, 277-8581, Japan*

<sup>4</sup>*Condensed Matter Research Center and Photon Factory,  
IMSS, KEK, Tsukuba, Ibaraki 305-0801, Japan*

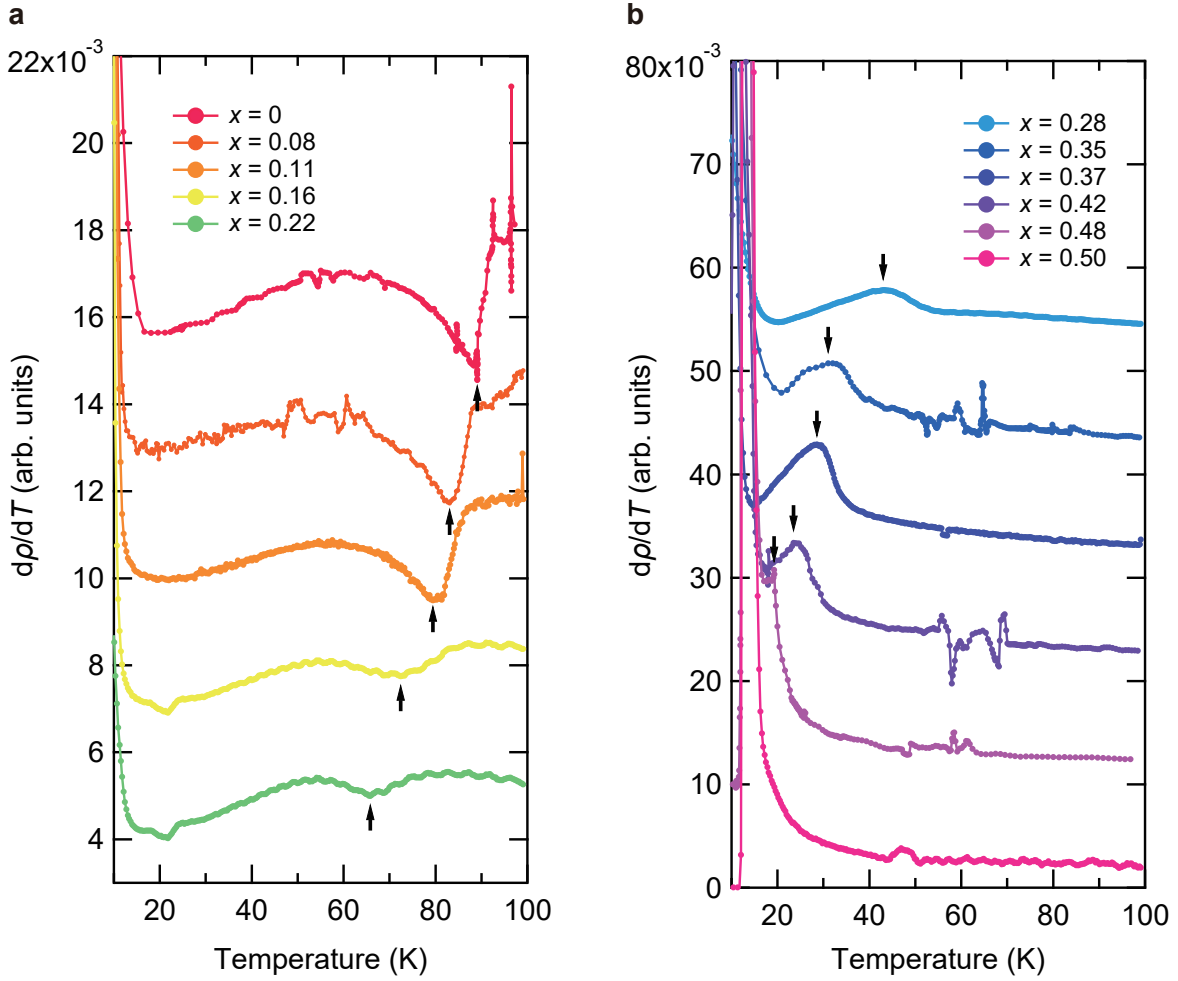
**Supplementary Fig. 1: Resistive determination of nematic transition temperature at ambient pressure.**

**Supplementary Fig. 2: Resistive determination of nematic and magnetic transition temperatures under pressure for  $x(\text{Te}) \approx 0.04$ .**

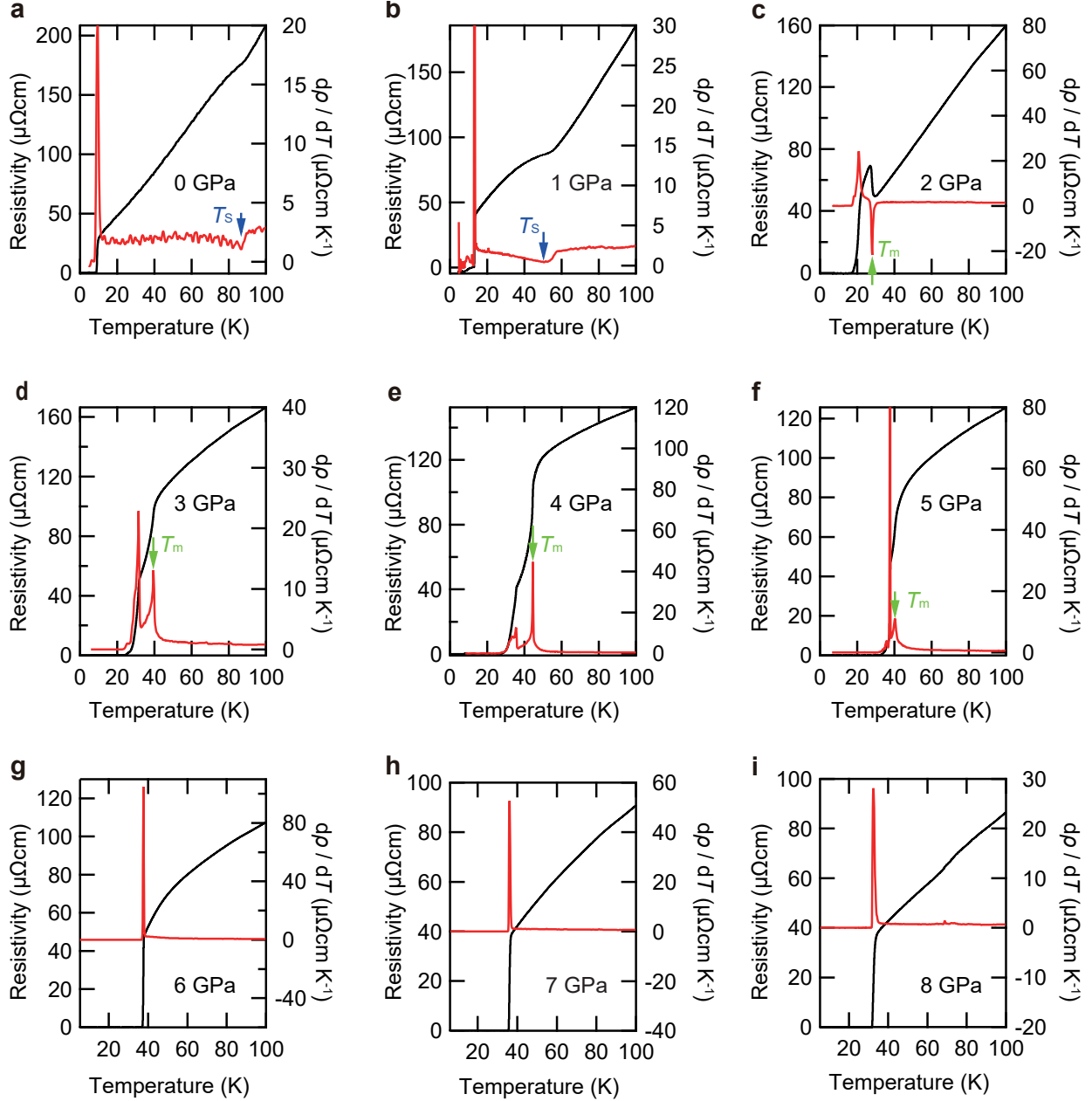
**Supplementary Fig. 3: Resistive determination of nematic and magnetic transition temperatures under pressure for  $x(\text{Te}) \approx 0.06$ .**

**Supplementary Fig. 4: Resistive determination of nematic and magnetic transition temperatures under pressure for  $x(\text{Te}) \approx 0.10$ .**

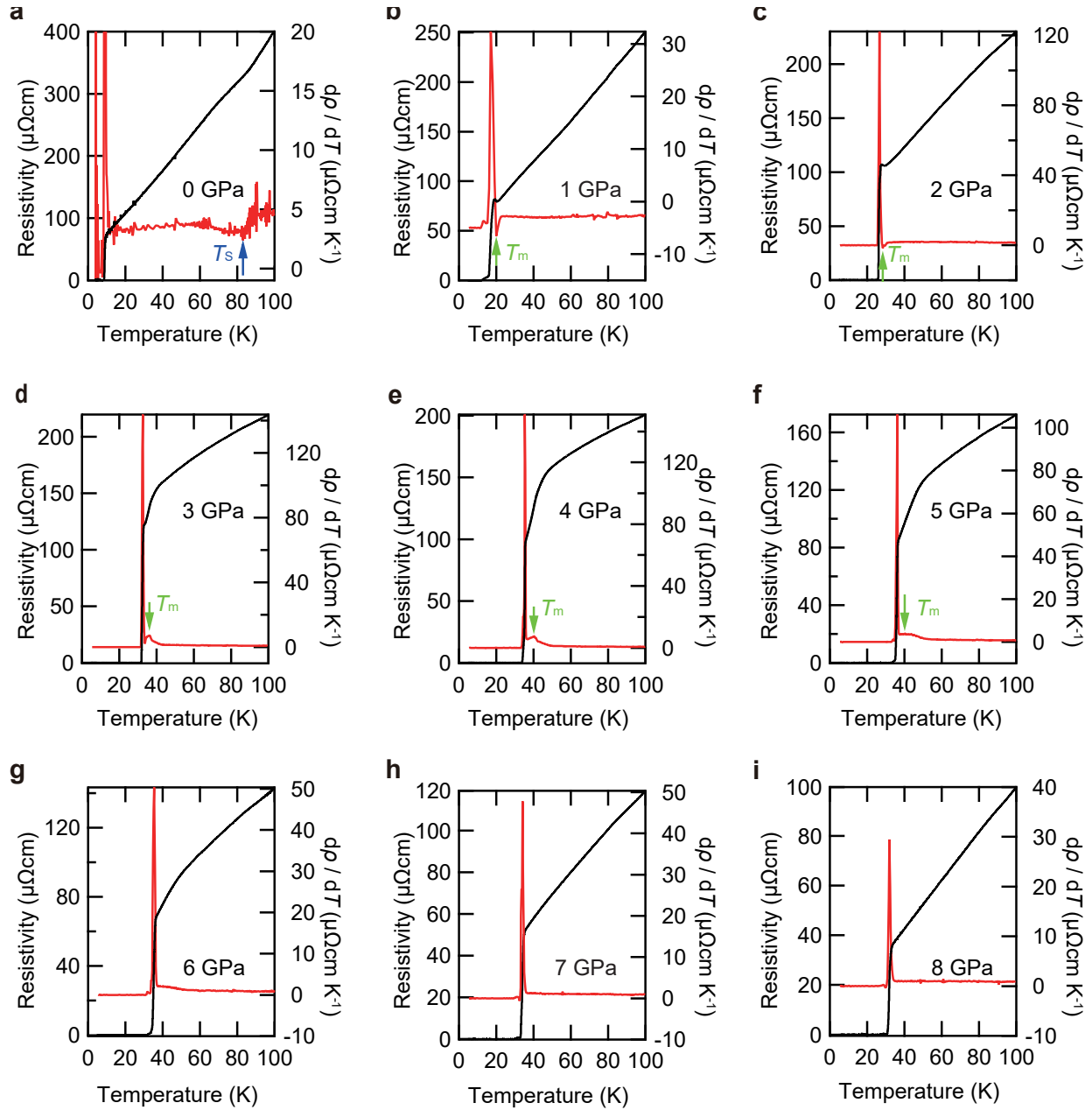
**Supplementary Fig. 5: Resistive determination of nematic transition temperature under pressure for  $x(\text{Te}) \approx 0.14$ .**



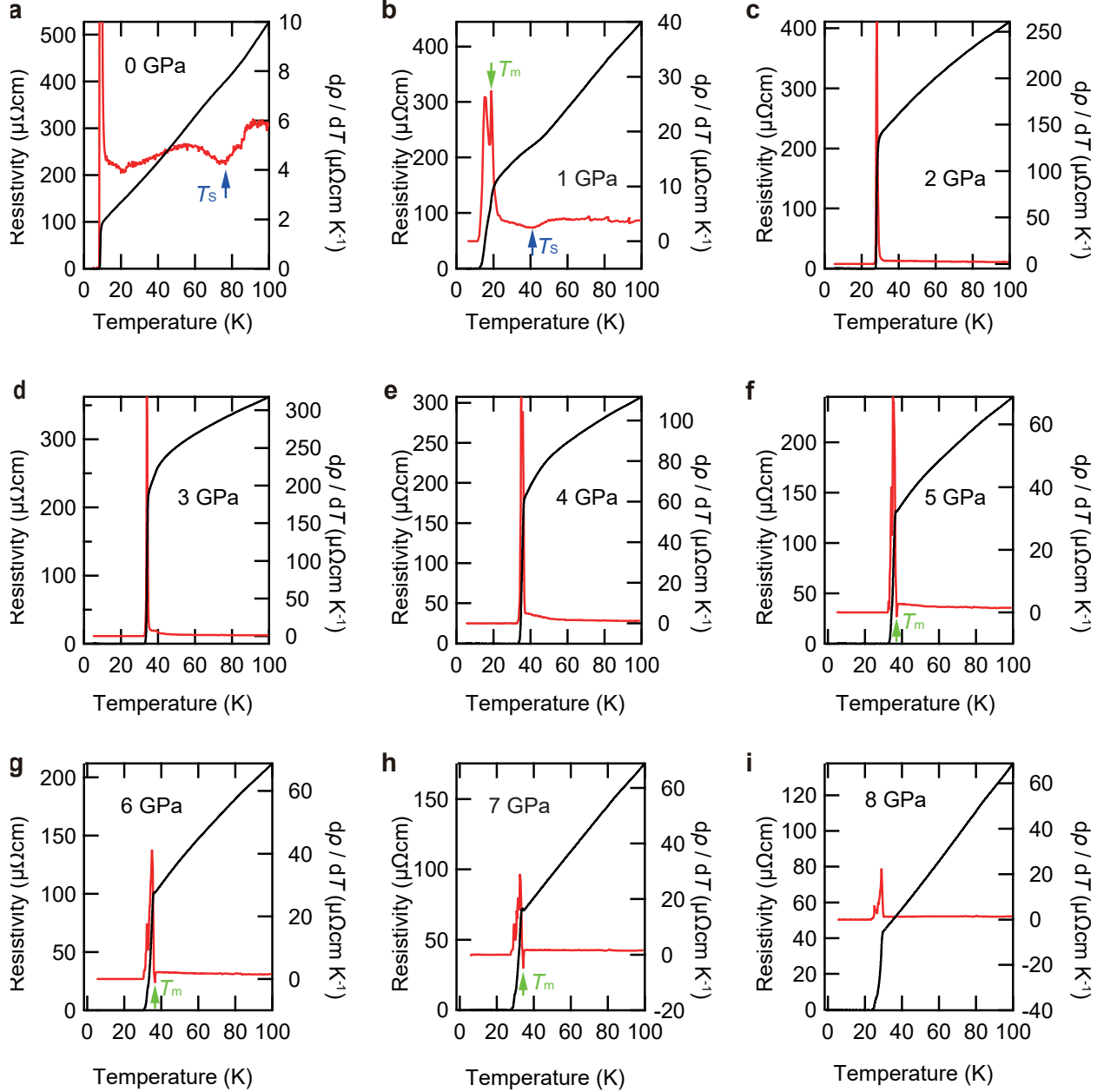
**Supplementary Fig. 1. Resistive determination of nematic transition temperature at ambient pressure.** **a**, Temperature dependence of  $d\rho/dT$  for  $0 \leq x(\text{Te}) \leq 0.22$  in  $\text{FeSe}_{1-x}\text{Te}_x$ . **b**, Temperature dependence of  $d\rho/dT$  for  $0.28 \leq x(\text{Te}) \leq 0.50$ . Data are shifted vertically for clarity. The arrows indicate the nematic transition temperature  $T_s$ . At  $T_s$  the temperature dependence of resistivity  $\rho(T)$  shows a kink anomaly with either upward or downward change depending on the condition. Thus we use dip or peak in the temperature derivative curves to define  $T_s$ .



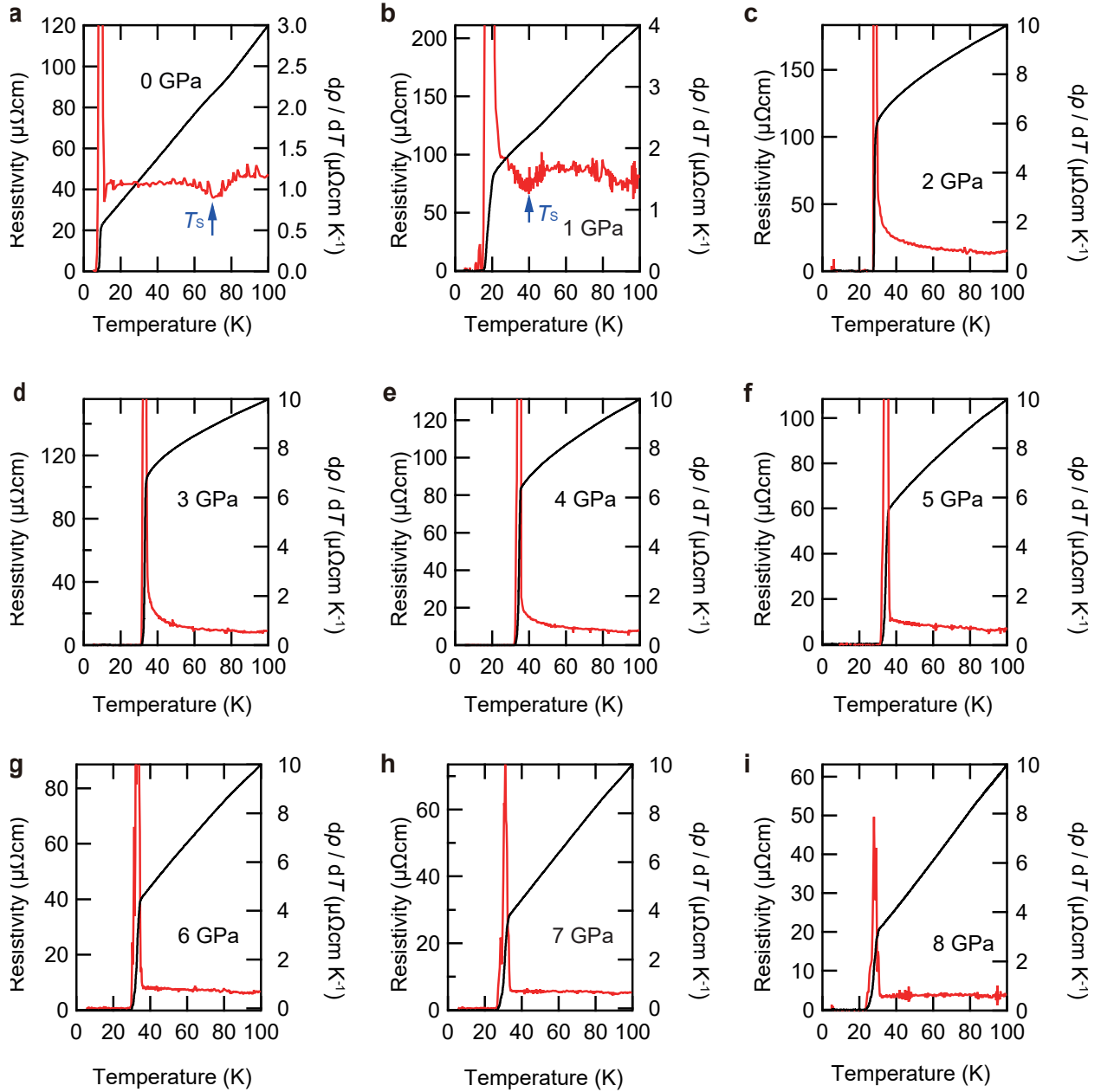
**Supplementary Fig. 2. Resistive determination of nematic and magnetic transition temperatures under pressure for  $x(\text{Te}) \approx 0.04$ .** **a-i**, Temperature dependence of resistivity  $\rho$  (black, left axis) and  $d\rho/dT$  (red, right axis) measured at 0-8 GPa with 1-GPa intervals. Arrows mark the nematic ( $T_s$ ) and magnetic ( $T_m$ ) transition temperatures.



**Supplementary Fig. 3. Resistive determination of nematic and magnetic transition temperatures under pressure for  $x(\text{Te}) \approx 0.06$ .** **a-i**, Temperature dependence of resistivity  $\rho$  (black, left axis) and  $d\rho/dT$  (red, right axis) measured at 0-8 GPa with 1-GPa intervals. Arrows mark the nematic ( $T_s$ ) and magnetic ( $T_m$ ) transition temperatures.



**Supplementary Fig. 4. Resistive determination of nematic and magnetic transition temperatures under pressure for  $x(\text{Te}) \approx 0.10$ .** **a-i**, Temperature dependence of resistivity  $\rho$  (black, left axis) and  $d\rho/dT$  (red, right axis) measured at 0-8 GPa with 1-GPa intervals. Arrows mark the nematic ( $T_s$ ) and magnetic ( $T_m$ ) transition temperatures.



**Supplementary Fig. 5. Resistive determination of nematic transition temperature under pressure for  $x(\text{Te}) \approx 0.14$ .** a-i, Temperature dependence of resistivity  $\rho$  (black, left axis) and  $d\rho/dT$  (red, right axis) measured at 0-8 GPa with 1-GPa intervals. Arrows mark the nematic ( $T_s$ ) transition temperatures.